Electronic Supplementary information

An Innovative Au-CdS/ZnS-RGO Architecture for Efficiently Photocatalytic Hydrogen Evolution

Shuangshuang Kai,[a] Baojuan Xi,[a] Xiaolei Liu,[b] Lin Ju,[b] Peng Wang,*[b] Zhenyu Feng,[a] Xiaojian Ma,[a] and Shenglin Xiong,*[a]

[a]Key Laboratory of the Colloid and Interface Chemistry, Ministry of Education, and School of Chemistry and Chemical Engineering, Shandong University, Jinan, 250100, P. R. China

[b]State Key Lab of Crystal Materials, Shandong University, Jinan, 250100, P. R. China

E-mail: pengwangicm@sdu.edu.cn, chexsl@sdu.edu.cn

Experimental section

Materials: Cadmium nitrate tetrahydrate ($Cd(NO_3)_2·4H_2O$, 99%, aladdin), zinc nitrate hexahydrate ($Zn(NO_3)_2·6H_2O$, 99%, Sinopharm), thiourea (TU, 99%, Sinopharm), Diethylenetriamine (DETA, 99%, Sinopharm), oleylamine (OLA, 80-90%, aladdin), hydrogen tetrachloroaurate (III) ($HAuCl_4·4H_2O$, ≥47.8%, Sinopharm), absolute ethanol (C_2H_5OH, AR, 99.7%, Tianjin Fuyu). All reagents were used in experiments as received without further purification.

Preparation of GO: Graphene oxide (GO) was prepared from natural graphite powder using the improved method (*ACS Nano* **2010**, *4*, 4806), and redispersed in ultrapure water for stock with the concentration of about 6.0 mg mL^{-1}.

Preparation of CdS/ZnS-RGO heterostructures (denoted as $Cd_xZn_{1-x}G_z$): CdS/ZnS-RGO was obtained by a facile one-pot hydrothermal method. In detail, 0.3 mmol $Cd(NO_3)_2·4H_2O$ and 0.7 mmol $Zn(NO_3)_2·6H_2O$ were dispersed in 35 mL ultrapure water and stirring for 1 h, followed by the addition of 2 mL of the stocked GO suspension. After stirring for 1 h and ultrasonication for another 1 h, the obtained mixture was kept stirring overnight. 0.1 g TU was added and stirred for 3 h. Then, the introduction of 1 mL DETA was applied and continuously stirred for another 2-3 h. Finally, the resultant suspension was transferred into a 50 mL Teflon-lined autoclave and maintained at 180 °C for 12 h. Via the centrifugation, the product was collected, washed with water and ethanol each for three times and freeze-dried for 3 days. The final sample prepared above is labeled as $Cd_{0.3}Zn_{0.7}G_2$, in which 0.3, 0.7 and 2 refer to 0.3 mmol $Cd(NO_3)_2·4H_2O$, 0.7 mmol $Zn(NO_3)_2·6H_2O$ and 2 ml GO, respectively. The following samples also accord with the nomination rule and generalized as $Cd_xZn_yG_z$ tuned by changing the molar amount of $Cd(NO_3)_2·4H_2O$ as well as $Zn(NO_3)_2·6H_2O$ and the volume of GO suspension.

The self-standing CdS and CdS/ZnS (denoted as Cd_xZn_y for convenience of comparison with $Cd_xZn_yG_z$) samples were prepared based on the above procedures except no addition of GO suspension.

Preparation of Au-CdS/ZnS-RGO: 50 mg of the as-prepared $Cd_{0.3}Zn_{0.7}G_2$ and a

certain amount (1, 2, 5 mg) of $HAuCl_4 \cdot 4H_2O$ were dissolved into 10 mL OLA in a three-neck round bottom flask under magnetic stirring and heated at 100 °C for 30 min under the N_2 atmosphere. The resulting product was collected by centrifugation and washed with hexane and ethanol for several times and finally freeze-dried for 3 days. The obtained sample was labeled as Au_z-$Cd_{0.3}Zn_{0.7}G_2$, where z means the mass of $HAuCl_4 \cdot 4H_2O$ applied.

Characterization: X-ray diffraction (XRD) patterns were obtained from an X-ray powder diffractometer (Bruker D8 Advance, Germany) with monochromatic Cu Kα as a radiation source. FESEM images were collected on a GeminiSEM 500 scanning electron microscope. Transmission electron microscopy (TEM) images were acquired by TEM (JEM-1011) at an accelerating voltage of 100 kV. TEM, HRTEM, HAADF-STEM, and EDX mappings were collected on on FEI Talos F200X TEM at 200 kV. Raman spectra were recorded on a JY LABRAM-HR confocal laser micro-Raman spectrometer with a 514.5 nm wavelength at room temperature. UV-Vis absorption spectra were recorded in the range of 250–900 nm at room temperature using a Shimadzu UV-2450 spectrometer. The steady-state photoluminescence (PL) spectra were using F-4500 (Hitachi Analytical Instruments). The electrochemical impedance spectroscopy (EIS) were measured on a electrochemical workstation (CHI 760E, Shanghai Chenhua, China) by using a conventional three-electrode quartz cell in which platinum sheet used as counter electrode and a saturated calomel electrode used as reference electrode, an 0.5 M K_2SO_4 aqueous solution was used as the electrolyte. The EIS Nyquist plots was obtained with a frequency range varied from 0.05 Hz to 100 kHz and the amplitude was set at 10 mV.

Photocatalytic hydrogen production activity: The photocatalytic H_2 production test was conducted in a 250ml round-bottom flask with 100ml aqueous solution containing 0.35 M Na_2S and 0.25 M Na_2SO_3. 10 mg of various as-prepared photocatalysts was added. A 300 W Xenon lamp equipped with a 420 nm UV cut-off filter was used to provide the visible light, which was positioned about 20 cm away from the flask reactor with the irradiation area and mean intensity of 24 cm^2 and ~140

mW cm^{-2} measured by PL−MW2000 spectroradiometer (Perfect Light, China). Before irradiation, the solution with photocatalyst was bubbled for 30 min with high-purity nitrogen to ensure oxygen-free condition and then stirred for several minutes to obtain homogenous mixture. The reaction was kept magnetic stirring at 15 °C. The amount of H_2 produced was determined using a gas chromatography (GC-7806) equipped with TCD detector (N_2 as carrier gas).

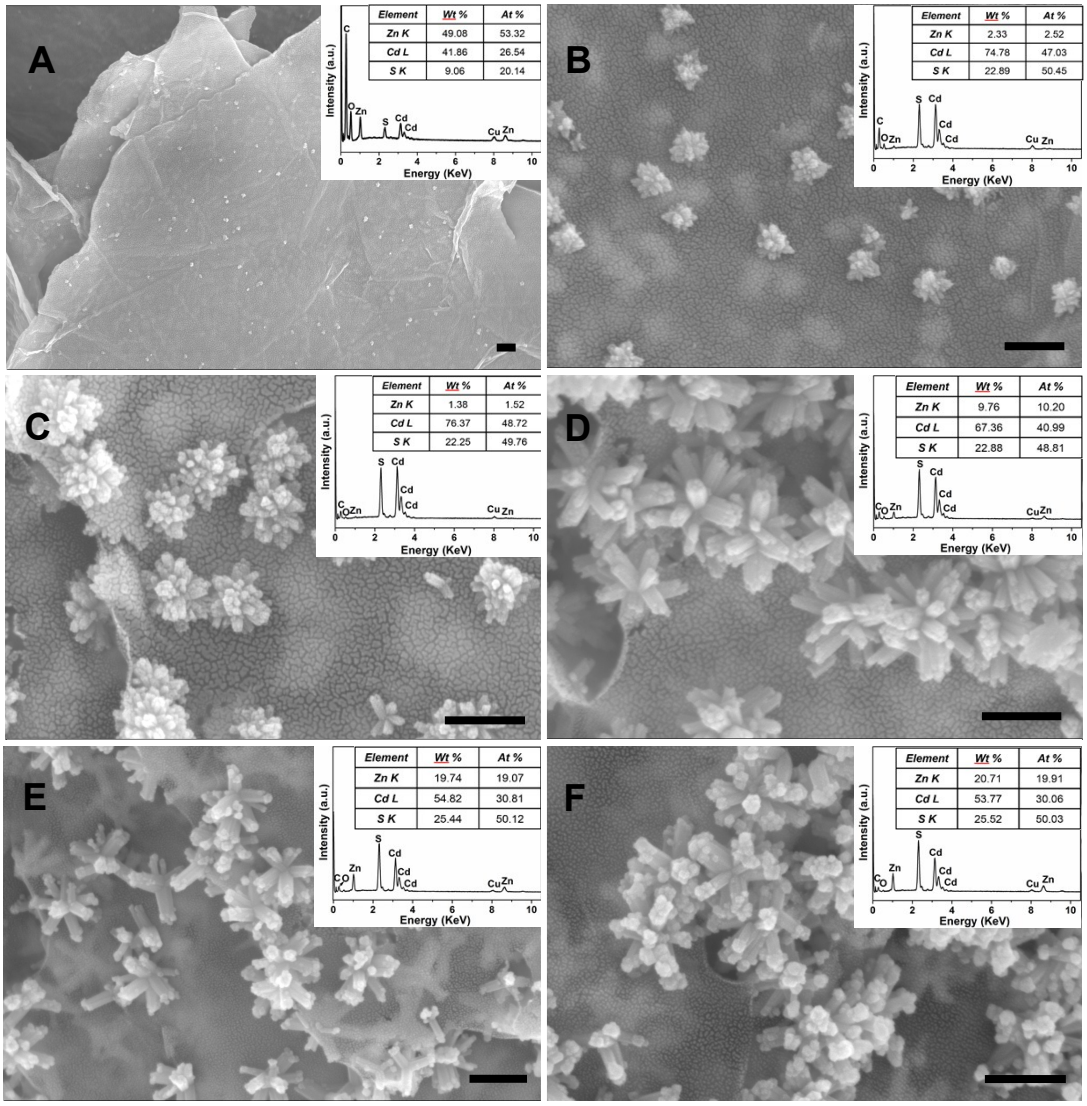

Figure S1. FESEM images and EDX spectra of intermediates for synthesis of $C_{0.5}Z_{0.5}G_2$ collected at 180 ºC (A) 0 h, (B) 0.5 h, (C) 1 h, (D) 1.5 h, (E) 6 h, (F) 12 h. Scale bars: 200 nm for all panels.

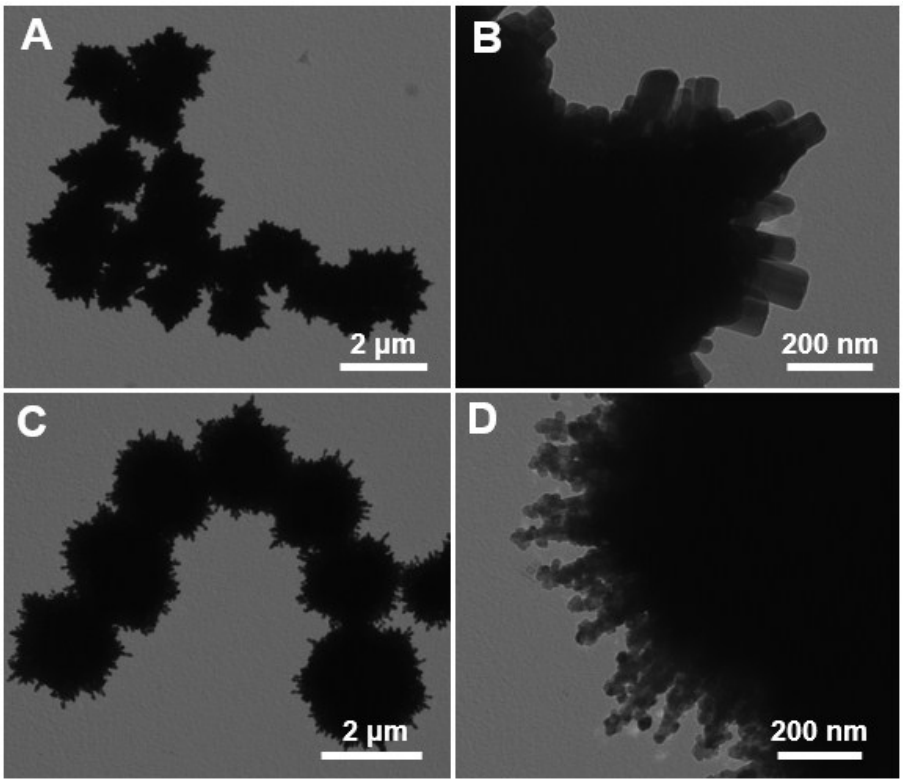

Figure S2. TEM images of (A, B) self-standing CdS and (C, D) $Cd_{0.3}Zn_{0.7}$ without the addition of graphene during the synthesis.

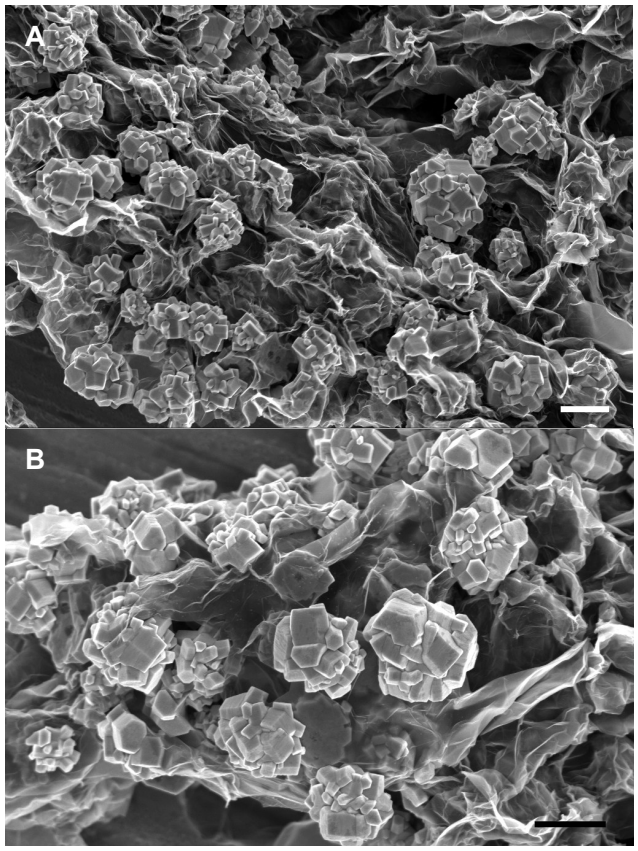

Figure S3. FESEM images of pure CdS on graphene prepared without DETA.

Note: In order to shed light on the growth process of CdS/ZnS-RGO, some control experiments were applied. Figure S2 shows TEM images of self-standing CdS and $Cd_{0.3}Zn_{0.7}$ prepared under the similar experimental process to $Cd_xZn_{1-x}G_2$ just without the application of graphene. CdS product is consisting of nanorods stacking tightly and $Cd_{0.3}Zn_{0.7}$ resembles with the addition of some nanoparticles attached around the nanorod stem. It's obviously that samples prepared are also nanorod assemblages, much bigger than their respective counterparts prepared in presence of graphene. In case of no DETA, it was found that only big-sized CdS aggregates were obtained on graphene sheets instead of nanorod bundles (see Figure S3). Hence, the presence of DETA plays a vital role in mediating the growth of 1D nanorod. With graphene as substrate, the formation of CdS/ZnS heterostructures was controlled by heterogeneous nucleation, in conjunction with DETA serving as structural direction agent to dominate the formation of 1D CdS nanorods. The time-dependent intermediates are also detected by SEM-EDX characterization to give information with $Cd_{0.5}Zn_{0.5}G_2$ as a sampling example. As the electric oven heated

from room temperature to 180 ^{o}C and the reaction immediately quenched, the sample was harvested for SEM testing. From Figure S1A, solid nanoparticles has already been anchored and EDX result justifies the absorption of Zn and Cd ions on RGO sheets. At 0.5 and 1.0 h of the reaction, it's obvious that CdS nanorod bunches are growing bigger. Zn content sharply decreases from EDX spectrum in Figure S1B-C due to the rapid growth of CdS crystals. Till 1.5 h, Zn content in EDX result begins to increase in Figure S1D, suggesting the formation of few ZnS nuclei. At 6 h, it can be clearly observed that some nanoparticles are capping on CdS nanorods and the relative atomic ratio of Zn to Cd also notably becomes larger, as proved by EDX result in Figure S1E. As the reaction extends to 12 h, ZnS particle aggregates grow bigger (see Figure S1F). As a result, the formation mechanism was proposed as follows. Ions of Cd and Zn are anchored on RGO sheets relying on the electrostatic interaction. By reaction with thiourea, CdS nuclei formed from solution readily depending on the heterogeneous nucleation. The crystal growth of CdS was dominated by DETA into hexagonal nanorods by combination with the inherent nature of hexagonal CdS, followed by heterogeneous growth of cubic ZnS phase greatly depending on the low lattice mismatching of h-CdS and c-ZnS.

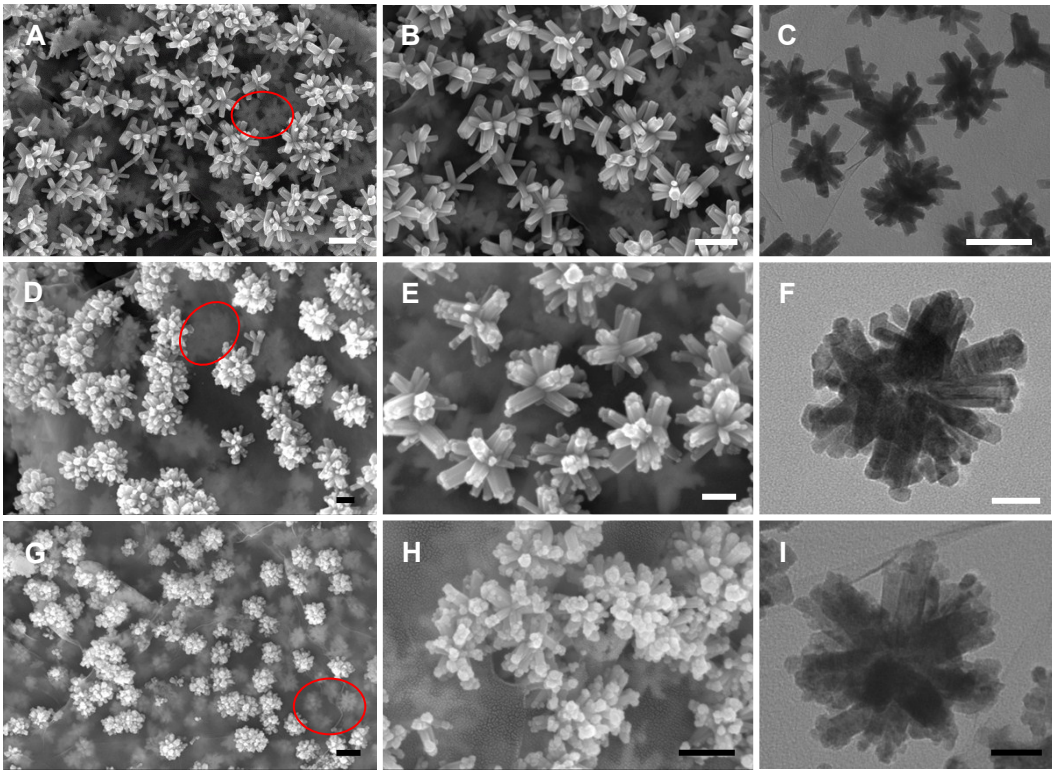

Figure S4. TEM and FESEM images of (A-C) $Cd_{1.0}Zn_0G_2$, (D-F) $Cd_{0.7}Zn_{0.3}G_2$, (G-I) $Cd_{0.5}Zn_{0.5}G_2$. scale bar: (A,B) 300 nm, (C,H,G) 200 nm, (D,E) 100 nm, (F,I) 50 nm.

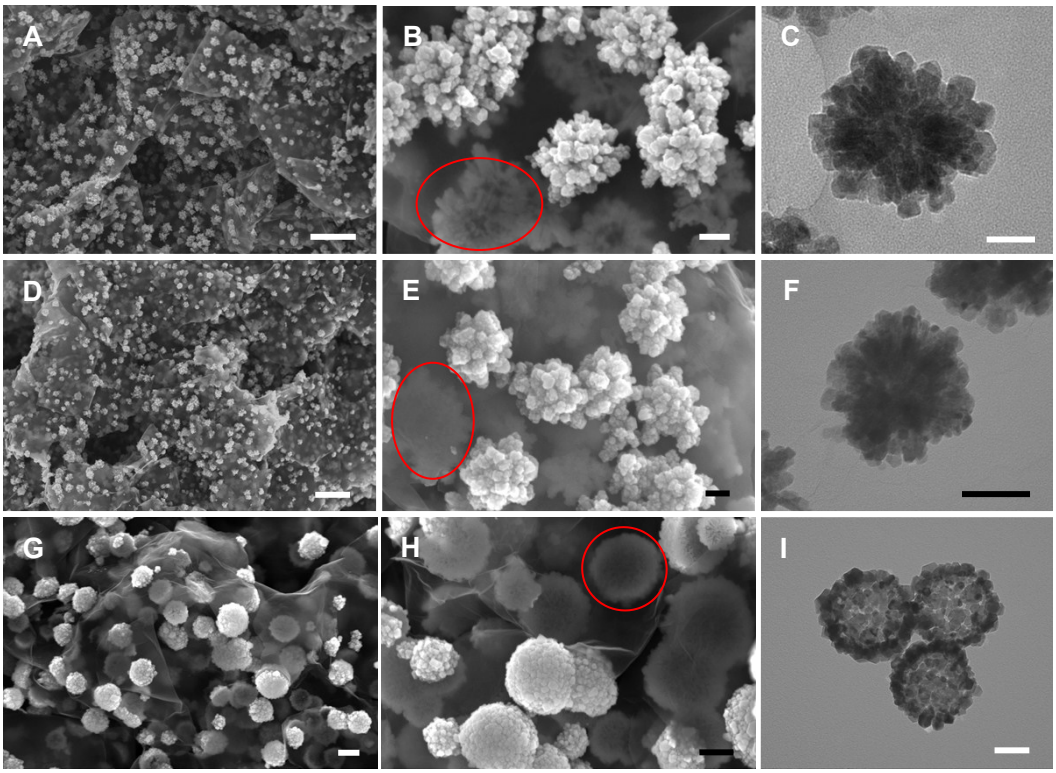

Figure S5. TEM and FESEM images of (A-C) $Cd_{0.3}Zn_{0.7}G_2$, (D-F) $Cd_{0.2}Zn_{0.8}G_2$, (G-I) $Cd_0Zn_{1.0}G_2$. Scale bar: (A,D) 1 μm, (B,E,F,I) 100 nm, (C) 50 nm, (G,H) 200 nm.

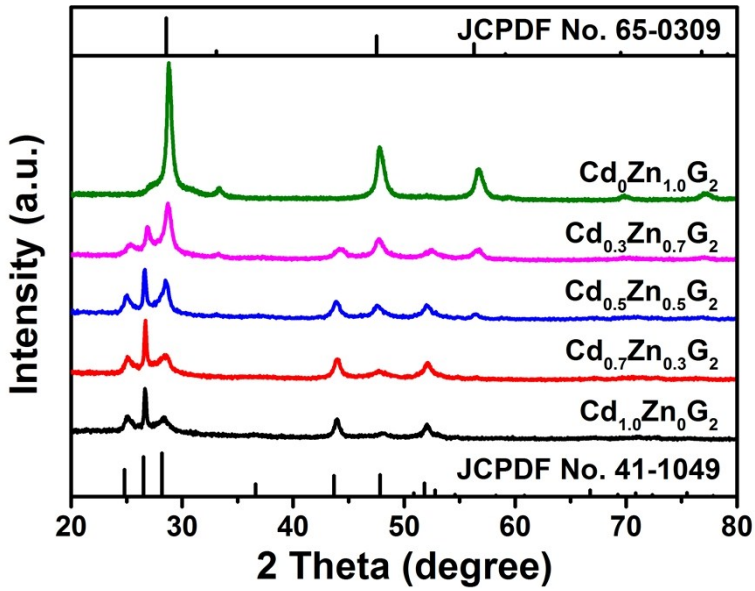

Figure S6. XRD patterns of $Cd_xZn_{1-x}G_2$ samples with different Cd : Zn molar ratio.

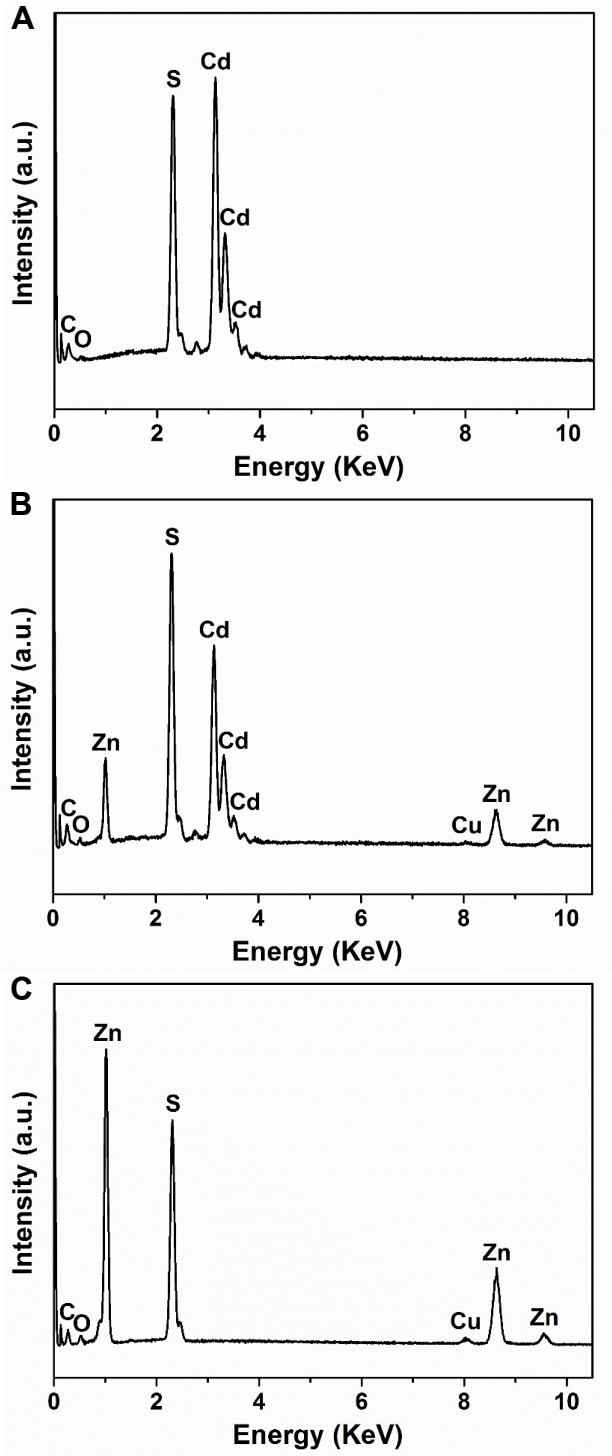

Figure S7. The EDX spectra of $Cd_{1.0}Zn_0G_2$, $Cd_{0.5}Zn_{0.5}G_2$ and $Cd_0Zn_{1.0}G_2$.

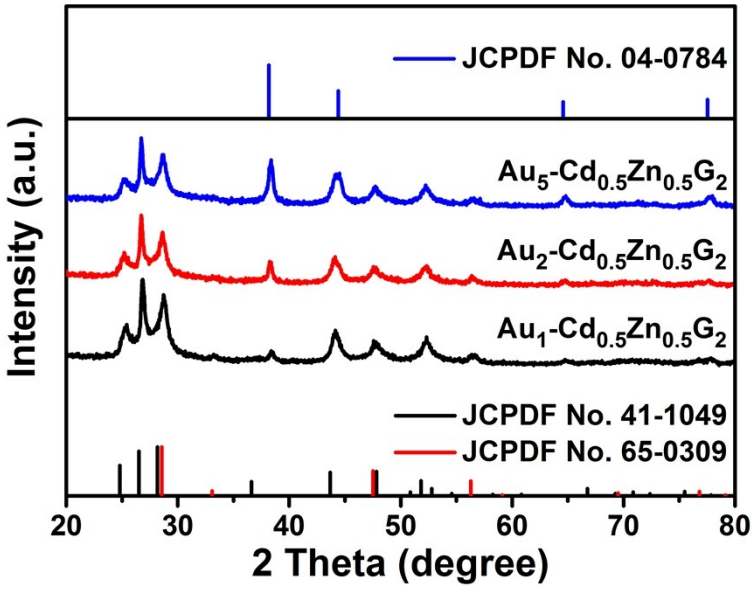

Figure S8. XRD patterns of Au_z-$Cd_{0.5}Zn_{0.5}G_2$ with different z values.

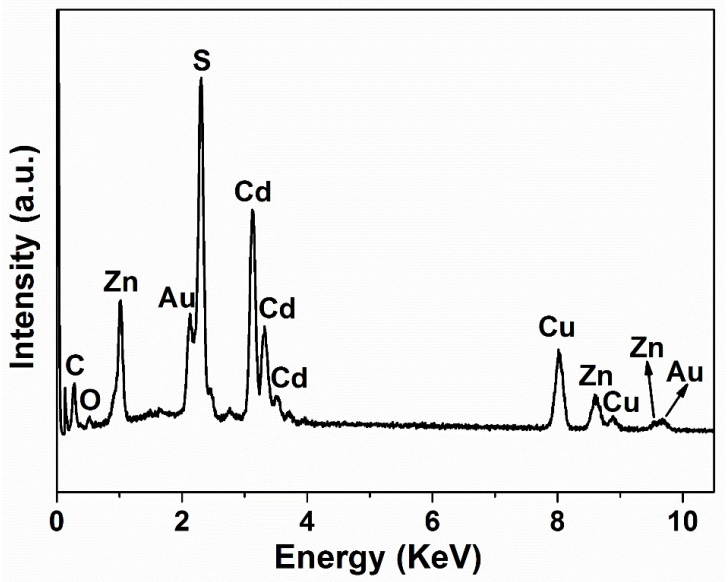

Figure S9. EDX spectrum of the as-prepared Au_2-$Cd_{0.5}Zn_{0.5}G_2$ composite.

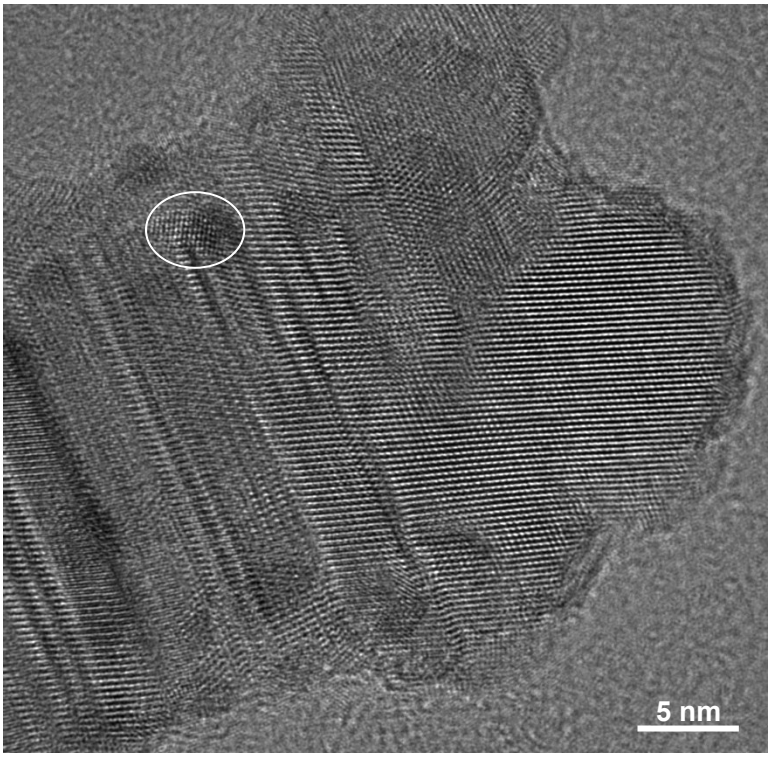

Figure S10. HRTEM image of a typical nanorod of Au_2-$Cd_{0.5}Zn_{0.5}G_2$. (The circle marked is Au nanoparticle domain).

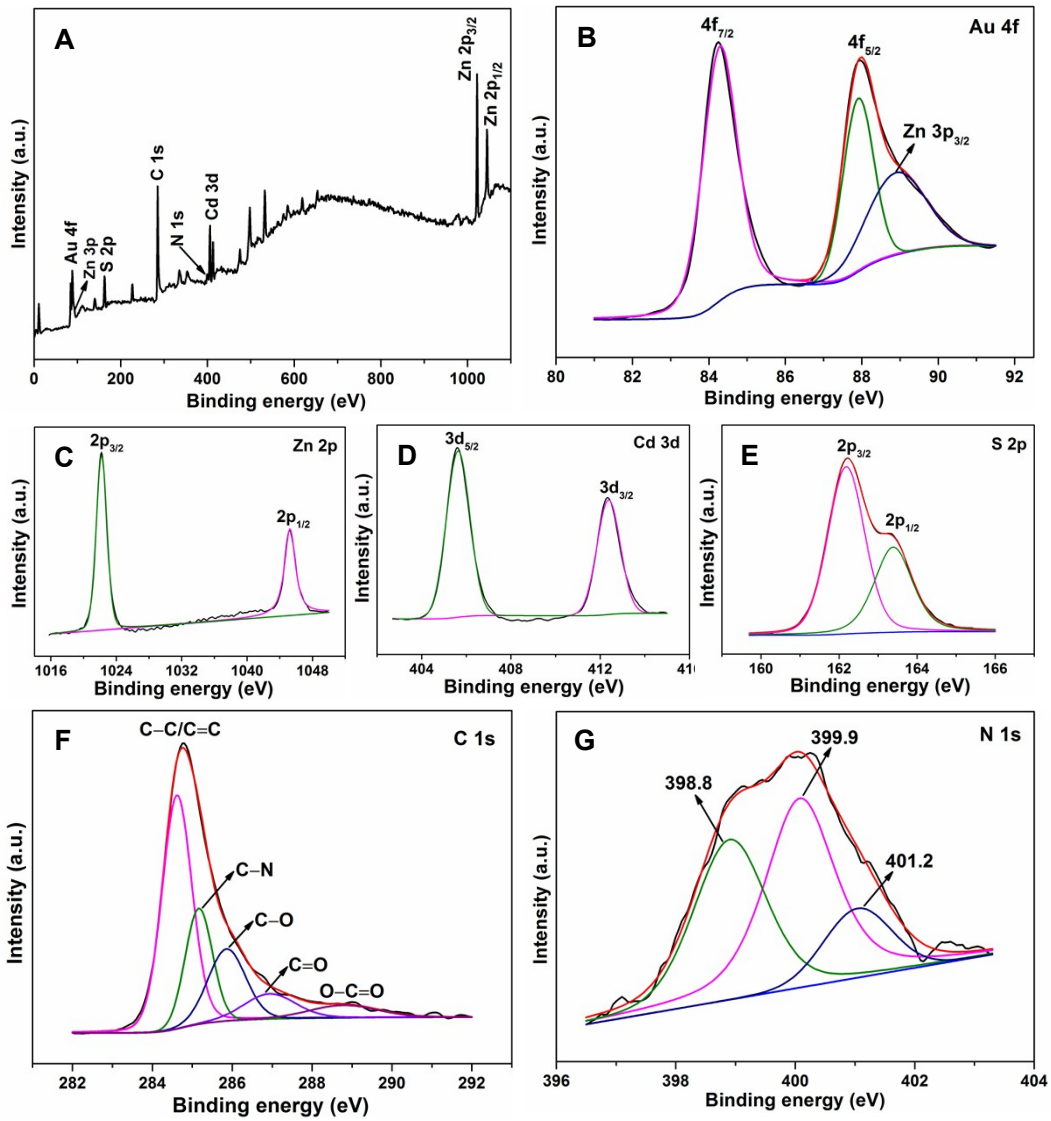

Figure S11. XPS spectra of (A) survey, (B) Au 4f, (C) Zn 2p, (D) Cd 3d, (E) S 2p, (F) C 1s and (G) N 1s.

Note: XPS technique was implied to detect the chemical state of elements in $Cd_{0.3}Zn_{0.7}G_2$-Au_2, whose survey spectrum (Figure S11A) displayed the chemical composition. The photoelectron spectrum of Au 4f in Figure S11B can be assigned to $4f_{7/2}$ and $4f_{5/2}$ located at 84.3 eV and 87.9 eV with a peak at 88.9 eV corresponding to Zn $3p_{3/2}$ orbit. In Figure S11C, Zn $2p_{3/2}$ and $2p_{1/2}$ peaks are located at 1022.2 and 1045.3 eV, displaying the valence of +2 for Zn. Cd 3d spectrum in Figure S 11D can be clearly identified as bands of $3d_{5/2}$ and $3d_{3/2}$ at 405.6 eV and 412.4 eV, respectively. As shown in Figure S11E, S $2p_{3/2}$ and $2p_{1/2}$ peaks center are located at

162.2 eV and 163.4 eV. High-resolution C 1s spectrum in Figure 11F includes C-C/C=C, C-N, C-O, C=O and O-C=O peaks located at 284.6 eV, 285.2 eV, 286.0 eV, 287.0 eV, and 288.8 eV, respectively. N 1s spectrum in Figure S11G can be deconvoluted into three peaks resulting from pyridinic N, pyrrolic N and amino N with center as 398.8 eV, 399.9 eV and 401.2 eV, respectively.

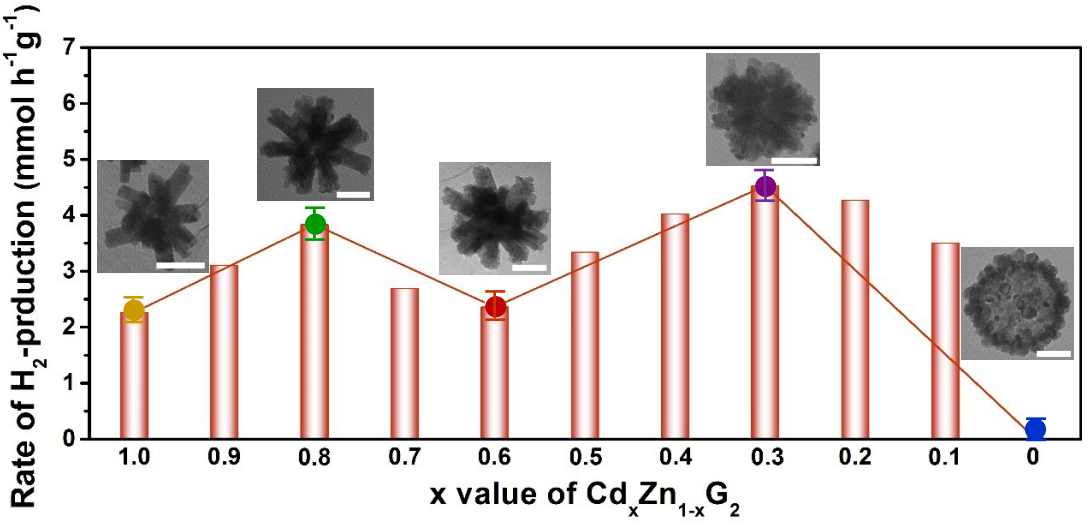

Figure S12. H_2 production rate under visible light irradiation of $Cd_xZn_{1-x}G_2$ with different x value for 1 h (inset scale bar: 100 nm).

Note: The change in H_2 production rate of $Cd_xZn_{1-x}G_2$ with different x value have a great relationship with the morphology features they evolved. Initially, the bare CdS nanorod bunches formed and then with the Zn/Cd ratio increasing the tip of CdS nanorod covered ZnS nanocrystals gradually, the first peak of H_2 production appeared as the tip of the nanorods covered entirely ($1.0 \geq x \geq 0.8$). Increasing the Zn/Cd ratio continuously the H_2 production going down, due to the ZnS nanocrystals on the tip is only grew bigger without increasing the contact area of heterojunction ($0.8 \geq x \geq 0.6$). The contact area of ZnS/CdS increasing with ZnS grow on both tip and side of the CdS nanorods, lead to the second peak of hydrogen production ($0.6 \geq x \geq 0.3$), excess ZnS caused another drop in the end ($0.3 \geq x \geq 0$).

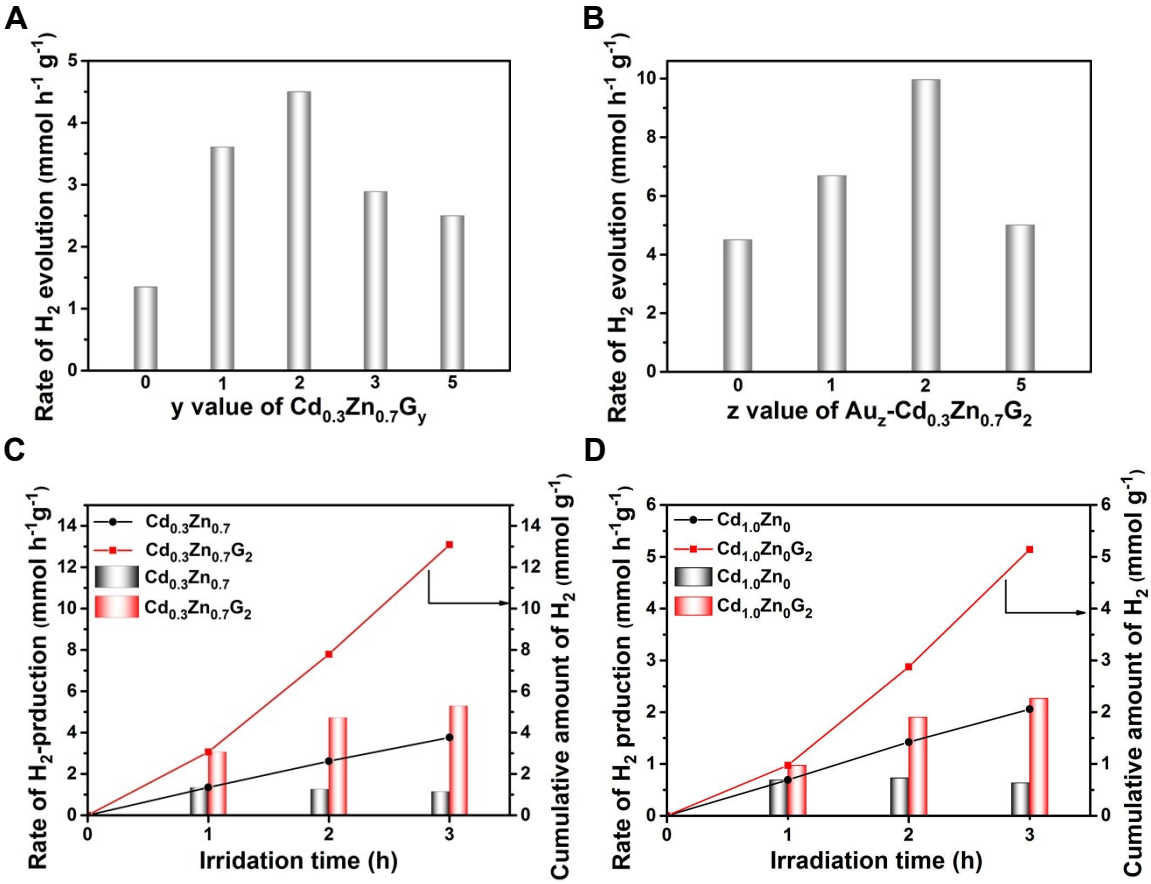

Figure S13. H_2 production rate under visible light irradiation of (A) $Cd_{0.3}Zn_{0.7}G_y$ with different y value for 1 h, (B) Au_z-$Cd_{0.3}Zn_{0.7}G_2$ with different z value for 1 h. The H_2 production rate in the initial 3 h of (C) $Cd_{0.3}Zn_{0.7}$ and $Cd_{0.3}Zn_{0.7}G_2$ as well as (D) $Cd_{1.0}Zn_0$ and $Cd_{1.0}Zn_0G_2$.

Note: Au_1-$Cd_{0.3}Zn_{0.7}G_2$ showed improved H_2 production rate, i.e. 6.68 mmol h^{-1} g^{-1}, compared with $Cd_{0.3}Zn_{0.7}G_2$. As increasing Au content, H_2 production rate of Au_2-$Cd_{0.3}Zn_{0.7}G_2$ was augmented to 9.96 mmol h^{-1} g^{-1}, 2.2 times that of $Cd_{0.3}Zn_{0.7}G_2$. Continual addition of Au rendered the declination of production rate over Au_5-$Cd_{0.3}Zn_{0.7}G_2$.

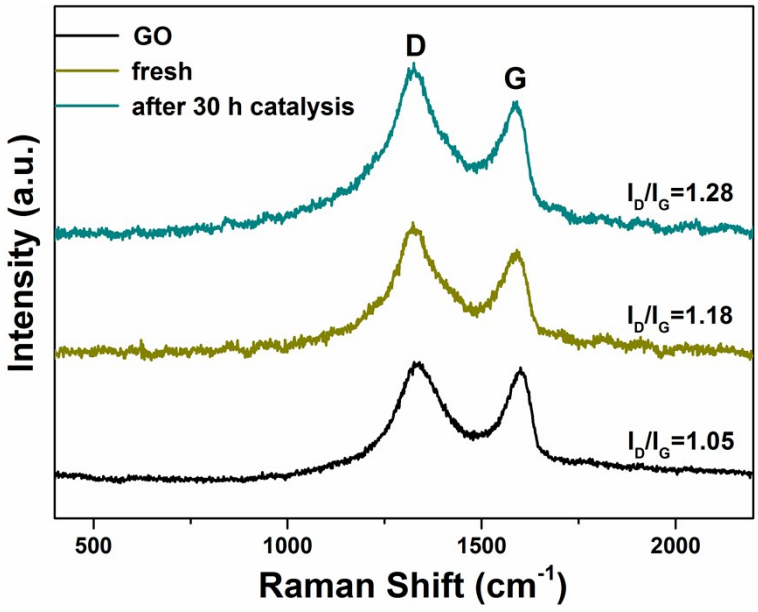

Figure S14. Raman spectra of GO, $Cd_{0.3}Zn_{0.7}G_2$ before and after 30 h catalytic H_2 production.

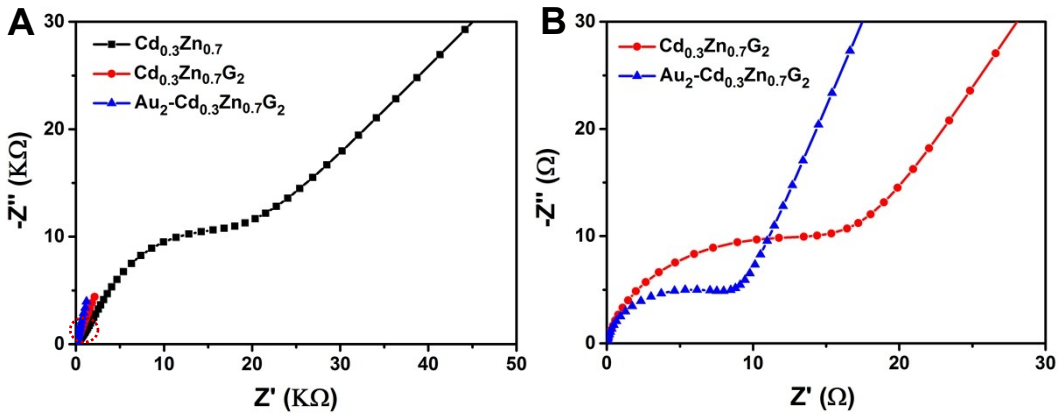

Figure S15. EIS Nyquist plots of $Cd_{0.3}Zn_{0.7}$, $Cd_{0.3}Zn_{0.7}G_2$, and Au_2-$Cd_{0.3}Zn_{0.7}G_2$ (Figure S15B is the part marked in Figure S15A).

Table S1. Comparative data of phototalytic H_2 production properties of CdS-related photocatalysts.

Photocatalyst	Incident light (nm)	Aqueous reaction solution	H_2 evolution rate (μmol h^{-1} g^{-1})	Stability (h)	Year (Ref.)
Au_2-$Cd_{0.3}Zn_{0.7}G_2$	**≥420**	**0.35 M Na_2S and 0.25 M Na_2SO_3**	**9960**	**30**	**This work**
$Cd_{0.3}Zn_{0.7}G_2$	**≥420**	**0.35 M Na_2S and 0.25 M Na_2SO_3**	**4500**	**30**	**This work**
CdS/ZnS	≥400	0.1 M Na_2S and 0.1 M Na_2SO_3	792	60	(2014)[1]
CdS/$Zn_{1-x}Cd_xS$	＞400	0.1 M Na_2S and 0.04 M Na_2SO_3	2128	N/A	(2010)[2]
CdS/ZnS	≥380	0.1 M Na_2S	N/A	N/A	(2013)[3]
$Cd_xZn_{1-x}S$	≥420	0.5 M Na_2S and 0.5 M Na_2SO_3	1667	15	(2012)[4]
$Zn_{0.8}Cd_{0.2}S$-RGO	≥420	0.35 M Na_2S and 0.25 M Na_2SO_3	1824	12	(2012)[5]
CdS/CNT/Pt	＞400	0.1 M Na_2S and 0.1 M Na_2SO_3	819	4	(2011)[6]
CdS/Pt/WO_3	＞400	lactic acid	2900	9	(2014)[7]
CdS/RGO-WO3	≥420	EtOH/H2O = 1:1, v/v	8528	20	(2016)[8]
WS_2–CdS	＞420	lactic acid	1984	16	(2015)[9]
MoS_2/RGO-CdS	＞420	lactic acid	9000	25	(2014)[10]
g-C3N4/CdS/NiS	≥420	triethanolamine	2563	12	(2015)[11]
NiS/$Zn_{0.5}Cd_{0.5}S$/RGO	≥420	0.35 M Na_2S and 0.25 M Na_2SO_3	375.7	12	(2014)[12]
CdS/Nb_2O_5/N-graphene	＞400	0.35 M Na_2S and 0.25 M Na_2SO_3	96.4	40	(2017)[13]
Au–Pt–CdS	＞420	0.35 M Na_2S and 0.25 M Na_2SO_3	778	12	(2016)[14]
Au-CdS/ZnS	≥400	0.35 M Na_2S and 0.25 M Na_2SO_3	675	N/A	(2015)[15]
$Cu_{1.94}S$−$Zn_{0.23}Cd_{0.77}S$	＞420	0.1 M Na_2S and 0.1 M Na_2SO_3	7735	20	(2016)[16]
CdS/Co_9S_8	N/A	Na_2S and Na_2SO_3	1061.3	25	(2017)[17]

Improving multiple[a]: the ratio of H_2-production rate for the optimal catalyst to pure CdS.

References

1 Y. P. Xie, Z. B. Yu, G. Liu, X. L. Ma, H.-M. Cheng, *Energy Environ. Sci.* 2014, ***7***, 1895.

2 J. Yu, J. Zhang, M. Jaroniec. *Green Chem.* 2010, ***12***, 1611.

3 L. Huang, X. Wang, J. Yang, G. Liu, J. Han, C. Li, *J. Phys. Chem. C,* 2013, ***117***, 11584.

4 Y. Yu, J. Zhang, X. Wu, W. Zhao, B. Zhang, *Angew. Chem. Int. Ed.* 2012, ***51***, 897.

5 J. Zhang, J. Yu, M. Jaroniec, J. R. Gong, *Nano Lett*., 2012, ***12***, 4584.

6 Y. K. Kima, H. Park, *Energy Environ. Sci.* 2011, ***4***, 685.

7 L. J. Zhang, S. Li, B. K. Liu, D. J. Wang, T. F. Xie, *ACS Catal*. 2014, ***4***, 3724.

8 Y. Huang, Y. Liu, D. y. Zhu, Y. Xin, B. Zhang, *J. Mater. Chem. A,* 2016, ***4***, 13626.

9 J. Chen, X.-J. Wu, L. Yin, B. Li, X. Hong, Z. Fan, B. Chen, C. Xue, H. Zhang, *Angew. Chem. Int. Ed.* 2015, ***54***, 1210.

10 K. Chang, Z. Mei, T. Wang, Q. Kang, S. Ouyang, J. Ye, *ACS Nano*, 2014, ***8***, 7078.

11 J. Yuan, J. Wen, Y. Zhong, X. Li, Y. Fang, S. Zhang, W. Liu, *J. Mater. Chem. A*, 2015, ***3***, 18244.

12 J. Zhang, L. Qi, J. Ran, J. Yu, S. Z. Qiao, *Adv. Energy Mater.* 2014, ***4***, 1301925.

13 Z. Yue, A. Liu, C. Zhang, J. Huang, M. Zhu, Y. Du, P. Yang, *Appl. Catal. B* 2017, ***201***, 202.

14 L. Ma, K. Chen, F. Nan, J.-H. Wang, D.-J. Yang, L. Zhou, Q.-Q. Wang, *Adv. Funct. Mater.* 2016, ***26***, 6076.

15 T.-T. Zhuang, Y. Liu, M. Sun, S.-L. Jiang, M.-W. Zhang, X.-C. Wang, Q. Zhang, J. Jiang, S.-H. Yu, *Angew. Chem. Int. Ed.* 2015, ***127***, 11657.

16 Y. Chen, S. Zhao, X. Wang, Q. Peng, R. Lin, Y. Wang, R. Shen, X. Cao, L. Zhang, G. Zhou, J. Li, A. Xia, Y. Li, *J. Am. Chem. Soc.* 2016, ***138***, 4286.

17 B. Qiu, Q. Zhu, M. Du, L. Fan, M. Xing, J. Zhang, *Angew. Chem. Int. Ed.* 2017, ***129***, 2728.